

Enzyme Responsive Chiral Self-sorting in Amyloid-inspired Minimalistic Peptide Amphiphiles

Deepika Gupta,^a Ranjan Sasmal,^b Ashmeet Singh,^a Jojo P. Joseph,^a Chirag Miglani,^a Sarit S. Agasti^b and Asish Pal^{a,*}

^aInstitute of Nano Science and Technology, Sector 64, Mohali, Punjab, 160062 (India)

^bJawaharlal Nehru Centre for Advanced Scientific Research (JNCASR), Jakkur, Bangalore 560064 (India)

Email: apal@inst.ac.in

Table of Contents

1.	Materials and Methods	S-2
2.	Synthesis and Characterization of peptides and probes	S-3
3.	Self-assembly of peptides	S-7
4.	SAXS	S-9
5.	CD Spectroscopic analysis	S-10
6.	Thioflavin-T binding study	S-11
7.	FT-IR studies	S-11
8.	Formation of hydrogels	S-12
9.	UV-vis and Fluorescence spectroscopy	S-12
10.	Generation of seeds and seeded Supramolecular Polymerization	S-15
11.	Seed mediated growth studies with ThT binding	S-17
12.	Confocal Laser Scanning Microscopy	S-17
13.	Structured Illumination Microscopy details	S-18
14.	Enantioselective Enzymatic activity	S-19
15.	References	S-24

Materials and Methods: All the reagents and amino acids were purchased from Sigma or TCI; standard amino acids with *L* and *D* configuration were either purchased directly or synthesized as protected Fmoc amino acids with the standard side chain protection with >99% chiral purity.¹ Hexafluoro isopropanol (HFIP), Pyrene butyric acid, Fluorescein isothiocyanate (FITC) and Rhodamine B isothiocyanate (RBITC) were also purchased from Sigma and 7-hydroxy carboxylic acid was synthesized with already reported procedure.² C-terminal amide peptides and fluorescent probes were synthesized on a 0.1 mmol scale using Fmoc-Rink Amide MBHA resin (0.52 mmol/g loading) from NovaBiochem (EMD Millipore). All solvents were either synthesis or analytical grade and Milli-Q water was used throughout the studies.

Peptides were synthesized using a *Liberty Blue CEM*, Matthews, NC, USA microwave-assisted peptide synthesizer following standard microwave Fmoc-solid phase peptide protocols. Reverse phase HPLC was performed with *Waters* binary HPLC system, using Nucleodur analytical column (C₁₈ stationary phase, 5 μm, 4.6 × 250 mm). The sample was injected with auto sampler and detected by photodiode array (PDA) detector. Electrospray Ionization Mass Spectrometry (ESI/MS) was performed with *Waters Aquire QDa* detector in suitable scan mode. Typical cone voltage is 15V and capillary voltage is 0.8V.

CD spectra were recorded using *JASCO J-1500* Circular Dichroism Spectrometer, Easton, MD, USA. The peptide solution was added to demountable cells (0.1 mm path length, Hellma) and scanned for wavelength range from 190 nm to 400 nm with scan speed of 50 nm min⁻¹ at 20 °C. The reported spectra are the average of 3 scans.

Negative stained TEM was performed using *JEOL JEM 2100* with a Tungsten filament at an accelerating voltage of 120 kV. The sample (6 μL) was deposited on carbon coated copper grid, and stained with the aqueous solution of uranyl acetate (1%; w/v) for 2 min and the excess solution was wicked off with the filter paper. The TEM grid was dried overnight under reduced pressure.

AFM imaging was performed on a *Bruker multimode 8* scanning probe microscope. Aqueous sample was deposited on the silicon chip and after 5 min sample was dried under nitrogen. Images were recorded in tapping mode with silicon cantilever (*Bruker*). Typical scan rates were between 0.6 - 1.0 Hz.

UV measurements were made in *Shimadzu UV-2600* spectrophotometer. Fluorescence emission spectrums were recorded using FS5 spectrofluorometer from Edinburgh instruments. Spectrums were recorded with scan slit and offset slit of 2 nm each with dwell time of 0.1 s at 25 °C.

FTIR was recorded on Agilent CARY 620 FTIR spectrophotometer. Spectra for lyophilized samples were recorded using a KBr pellet. A freeze-dried sample was mixed with KBr to make the pellet. The background was collected using a blank KBr pellet. FT-IR of liquid samples of nanofibers were recorded in CaF₂ (Calcium fluoride) cell. Samples were dissolved in D₂O (conc. = 5 mM).

SAXS experiments were carried out on SAXSess mc² instrument (Anton-Paar) with line-collimation system using a Cu-K α source with wavelength of 1.54 Å. Perkin Elmer cyclone image plate recorder was used to record the data. SAXSQuant 2D software was used to reduce the two dimensional data to one dimensional, Intensity (I) vs scattering vector (q) plot. PDDF curves were obtained by using GIFT software.

The linear viscoelastic region, storage modulus, loss modulus and thixotropic studies were calculated using a Rheoplus 302 (advanced Rheometer) device using parallel plate (PP25) geometry at measuring distance of 0.1 mm at 25 °C.

Continuous amyloid growth assays were measured on multimode microtiter plate reader (BioTek synergy 2, Finland) using black standard 96-well plates.

Confocal laser scanning microscopy images were taken with LSM 880 (carl Zeiss) equipped with an confocal detector. The samples were excited with 488 and 561 lasers, respectively.

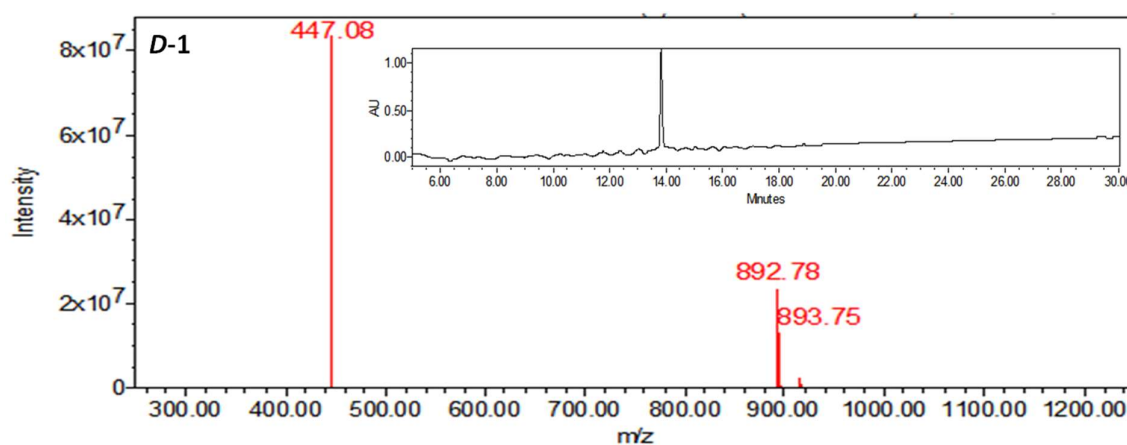
Structured illumination microscopy (SIM) was carried out using an inverted Zeiss ELYRA PS1 microscope. Two lasers have been used for excitation: 488 nm (200 mW) and 561 nm (200 mW) for respective excitation of fluorophores. Imaging was performed using a Zeiss oil-immersion objective (alpha Plan-apochromat DIC 63x/1.40 Oil DIC M27, numerical aperture (NA) 1.40 oil) using 100 ms exposure time and 5% of the laser power from both the lasers: 488 nm (26 w.cm⁻²) and 561 nm (22 w.cm⁻²). Fluorescence light was spectrally filtered with emission filters (MBS-488+EF BP 495-570/LP 750 for laser line 488 and MBS-561+EF BP 570-650/LP 750 for laser line 561) and imaged using a PCO edge sCMOS camera. The acquired images were processed using Zen 2.0 software and additional image analysis and color adjustment were carried out using ImageJ and Origin 9.0.

Synthesis and Characterization of peptides:

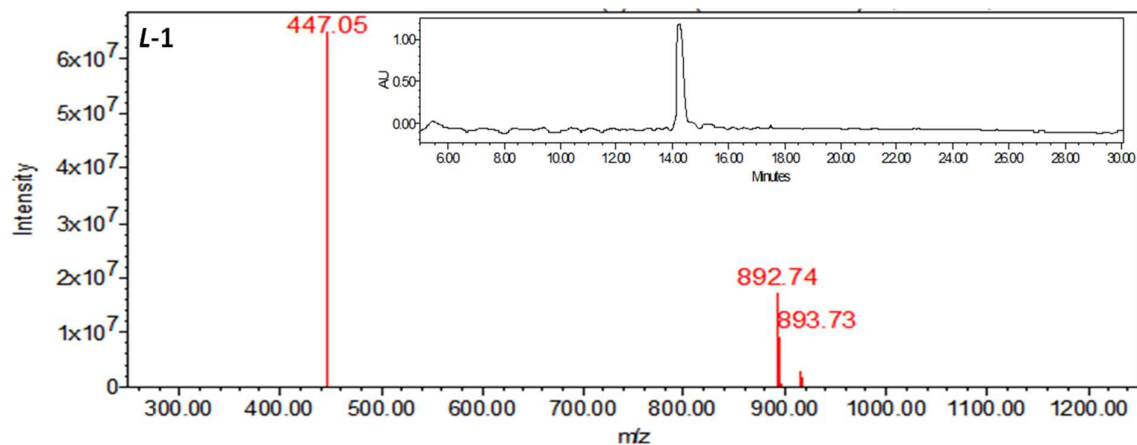
Peptides and fluorescent probes were synthesized on rink amide MBHA resin at 0.1 mmol scale following standard microwave Fmoc-solid phase peptide Synthesis (SPPS) protocols. Amino acids were coupled using diisopropyl carbodiimide (DIC) and oxyma in dimethylformamide (DMF). Fmoc deprotection was performed with 20% piperazine in DMF (containing 10%

ethanol) in microwave at 75 °C. Resin bound peptide was filtered, washed with DMF and dichloromethane and allowed to dry. The peptides were cleaved from the resin using 10 ml of cleavage cocktail mixture (trifluoroacetic acid (TFA)/triisopropylsilane (TIPS) / Water (95: 2.5: 2.5, v/v/v)). The mixture was shaken for 3 h at the room temperature followed by removal of the resin through filtration and the filtrate was concentrated to volume of approximately 1 ml. The resultant residue was precipitated by dropwise addition of ice cold diethyl ether. The precipitated product was centrifuged for 15 min at 7000 rpm at 4 °C. The precipitates were washed 3 times with cold diethyl ether and air dried. For synthesis of **D-4** and **L-5** probes, VFFA peptidyl-resins were coupled with Fmoc- amino hexanoic acid and were reacted with Rhodamine B isothiocyanate (RBITC) and Fluorescein isothiocyanate (FITC) respectively in excess of DIPEA.³ The peptides (**L-1** and **D-1**) were re-dissolved in CH₃CN/H₂O (1:9) to analyse purity of peptides by reverse phase HPLC with mobile phase acetonitrile and water containing 0.1% formic acid. To alleviate the chances for self-assembly during HPLC purification, the peptides in powder form were dissolved in HFIP and dried once again. The solid residue of fluorescent probes (**L-2**, **D-2**, **L-3**, **D-3**, **D-4** and **L-5**) were re-dissolved in DMSO and confirmed by ESI-MS and stored at -20°C. The standard gradient used for analytical HPLC for both peptides (**L-1** and **D-1**) was 5 → 95%CH₃CN in H₂O (0.1% HCOOH additive) with flow rate of 1 mL/min over 30 min. Injection volume for **L-2**, **D-2**, **L-3** and **L-3** is 5 µL (1 mM) with gradient method 70 → 95%CH₃CN in H₂O (Additive 0.1% HCOOH) over 15 min.

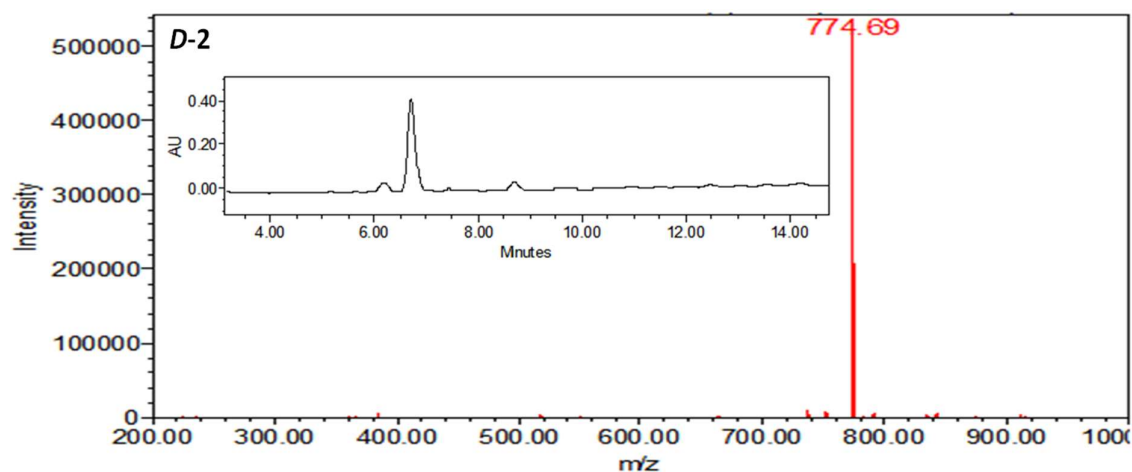
D-1: Calculated exact mass for C₄₈H₇₇N₉O₇ = 891.59, In positive mode: found [MH⁺] = 892.78, [MH₂]²⁺ = 447.08.



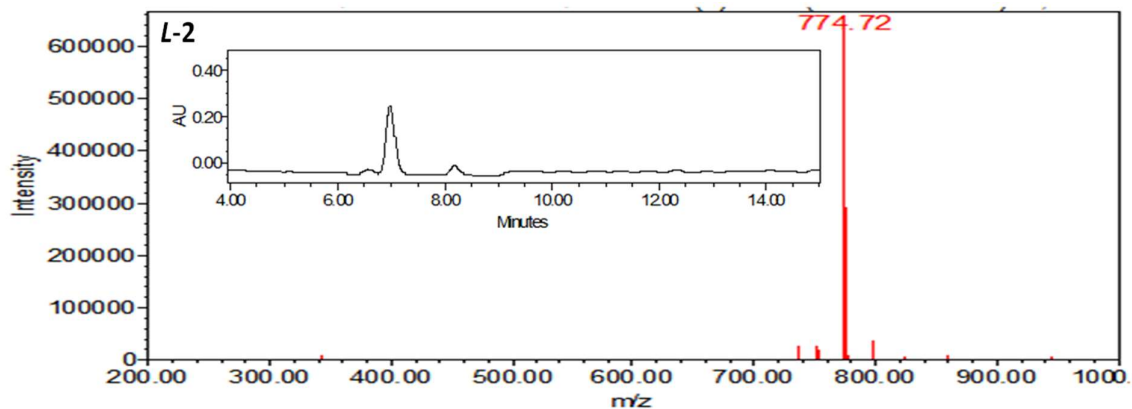
L-1: Calculated exact mass for $C_{48}H_{77}N_9O_7 = 891.59$, In positive mode: found $[MH^+] = 892.74$, $[MH_2]^{2+} = 447.05$



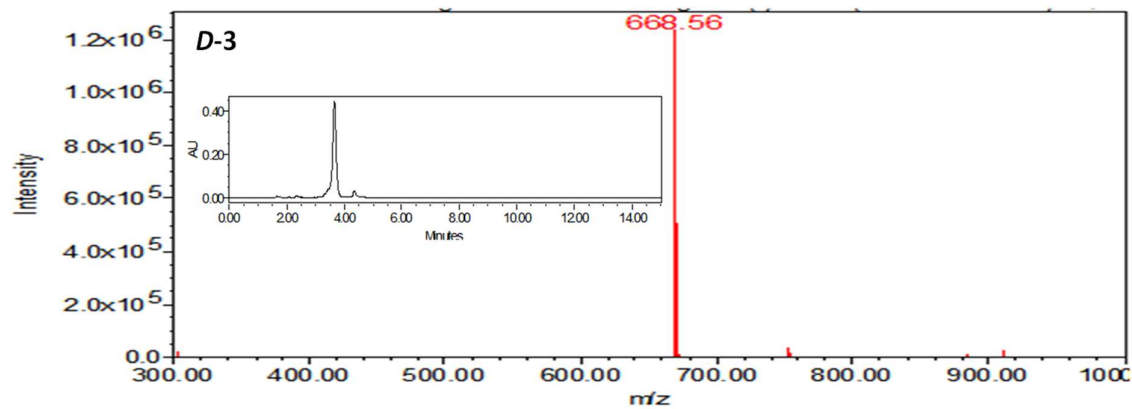
D-2: Calculated exact mass for $C_{46}H_{49}N_5O_5 = 751.37$, In positive mode: found $[M+Na]^+ = 774.69$



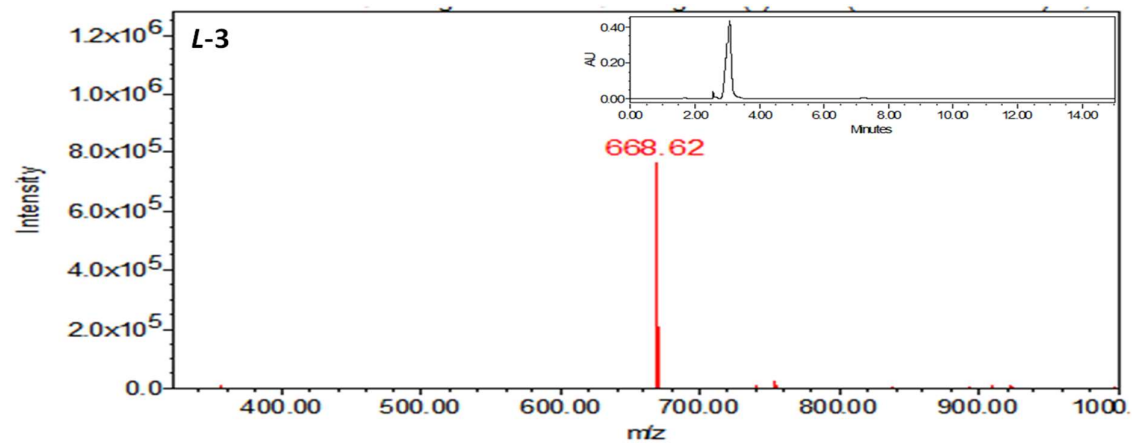
L-2: Calculated exact mass for $C_{46}H_{49}N_5O_5 = 751.37$, In positive mode: found $[M+Na]^+ = 774.72$



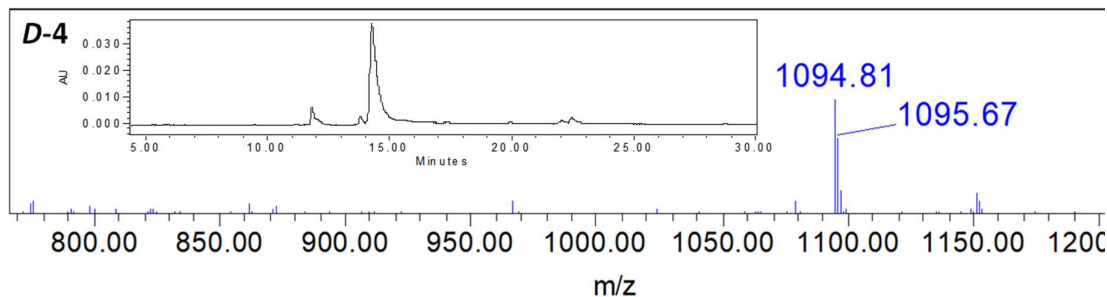
D-3: Calculated exact mass for $C_{36}H_{39}N_5O_8 = 669.28$, In negative mode found: $[M]^- = 668.56$



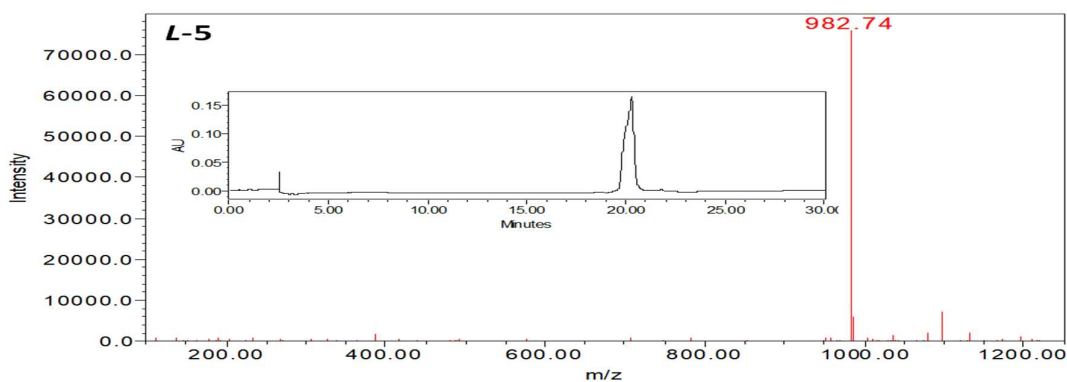
L-3: Calculated exact mass for $C_{36}H_{39}N_5O_8 = 669.28$, In negative mode found: $[M]^- = 668.62$



D-4: Calculated exact mass for $C_{61}H_{76}N_9O_8S = 1095.56$, In negative mode found: $[M]^- = 1094.81$.



L-5: Calculated exact mass for $C_{53}H_{57}N_7O_{10}S = 983.39$, In negative mode found: $[M]^+ = 982.74$.



Self-assembly of peptides:

Peptides (*L*-1 and *D*-1, conc. 2 mM) were taken in water or tris-HCl buffer (pH = 7.4) and mechanically agitated for 1-2 min to dissolve at room temperature. After incubation for a day, the formation of self-assembled peptide nanofibers mediated by hydrogen bonding and π - π interactions were confirmed by AFM and TEM images.

For hydrogel formation, higher concentration of the peptide amphiphiles (10 mM) was mechanically agitated to dissolve in sodium phosphate buffer (10 mM, pH 7.4). Upon incubating at room temperature for 1 day, the negatively charged phosphates electrostatically interact with the positively charged peptide nanofibers to render network structure to eventually result hydrogel.

Fluorescent probes are soluble in DMSO and does not form self-assembled nanostructures upon injecting DMSO stocks of the probes into water.

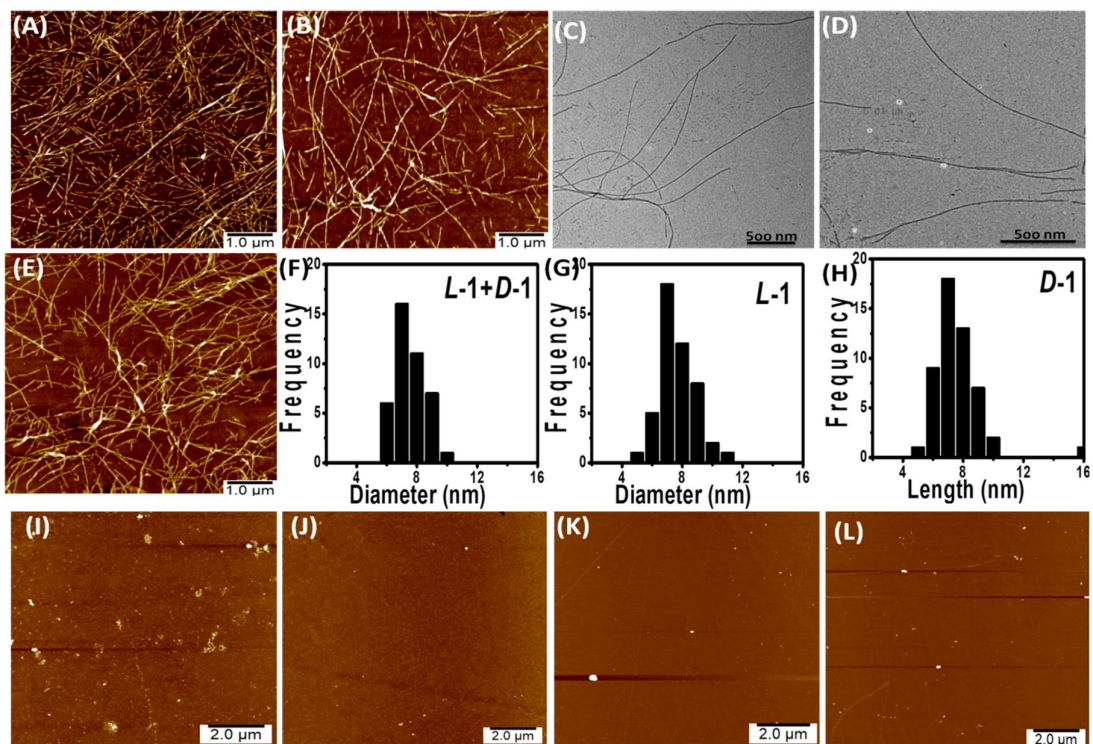


Figure S1 (I): AFM height images and TEM images of the peptide *L-1* (A,C) and *D-1* (B,D) in water at room temperature (conc = 1 μM for TEM and 100 μM for AFM). (E) AFM image of *L-1* and *D-1* peptide mixed in powder form followed by addition of water (solid phase mixing). (F,G,H) Histogram analyses for diameter distribution of the peptide amphiphiles. AFM images of fluorescent probes (1 mM) in water upon dilution from DMSO stock solution. (I) *L-2* (J) *D-2* (K) *L-3* and (L) *D-3* showed absence of supramolecular peptide nanofibers.

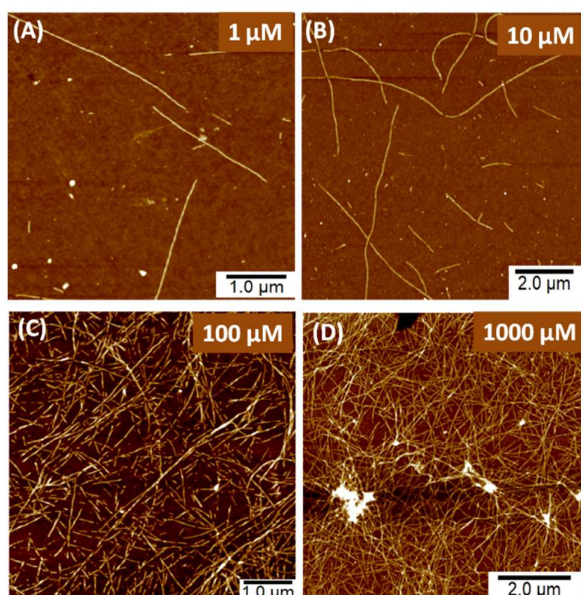


Figure S1 (II): AFM height images recorded for different concentrations of *L-1*. (A) 1 μM , (B) 10 μM , (C) 100 μM and (D) 1000 μM .

SAXS study:

Small angle X-ray scattering (SAXS) profiles obtained from kinetic nanofibers of peptides were fitted with a model for non-interacting long cylinders with a cylindrical form factor with a gaussian distribution of core radius. The fitting was carried out using SASfit software. Good fits were obtained for SAXS data with the cylindrical model fit having core and shell radii of $1.5 (\pm 0.2)$ nm and $1.9 (\pm 0.2)$ nm, respectively.

The intensity formula used to describe the fit for the SAXS data was

$$I = \int K_{\text{Cyl}}(Q, \eta_{\text{core}} - \eta_{\text{shell}}, R, L, x) + K_{\text{Cyl}}(Q, \eta_{\text{shell}} - \eta_{\text{solv}}, R + \Delta R, L, x)^2 dx$$

where $K_{\text{Cyl}}(Q, \Delta\eta, R, L, x) = 2\pi R^2 L \Delta\eta \left(\frac{J_1(QR\sqrt{1-x^2}) \sin(QLx/2)}{(QR\sqrt{1-x^2}) QLx/2} \right)$

Input Parameters for model core-shell long cylinder:

R: core radius of cylinder, ΔR : shell thickness, L: length of cylinder, $\Delta\eta$: scattering contrast

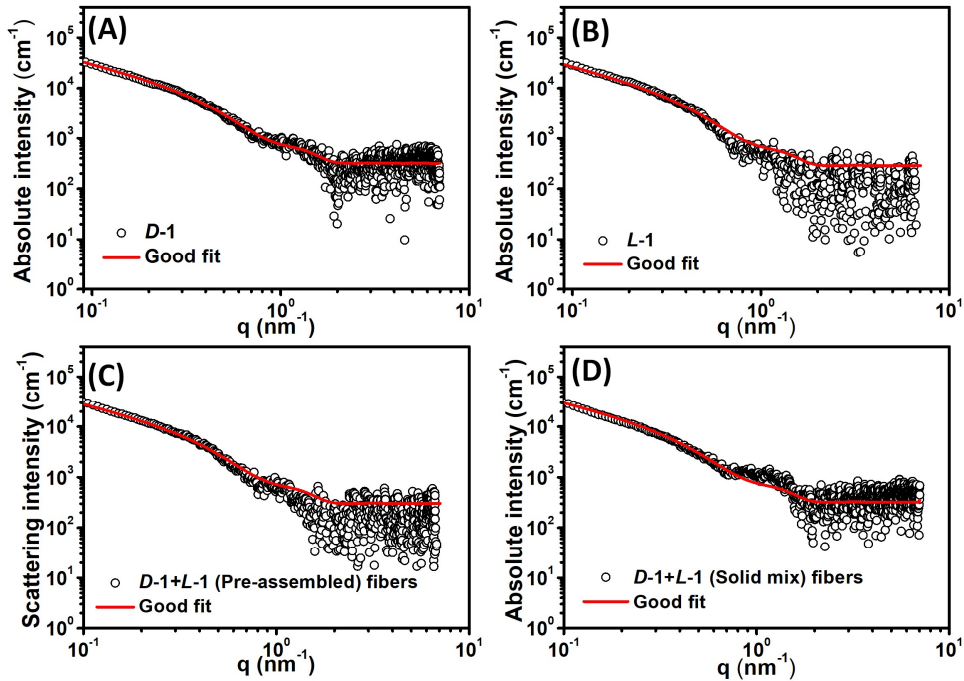


Figure S2: SAXS profile recorded at 25 °C in water for the individual (10 mM) (A) **D-1**, (B) **L-1**. SAXS profile for the mixture of peptide amphiphiles in 1:1 ratio (total concentration 10 mM). (C) Solution mixture of **D-1** and **L-1** fibers and (D) solid mixture **D-1** and **L-1** peptide followed by dissolution in water for self-assembly.

CD Spectroscopic Analyses:

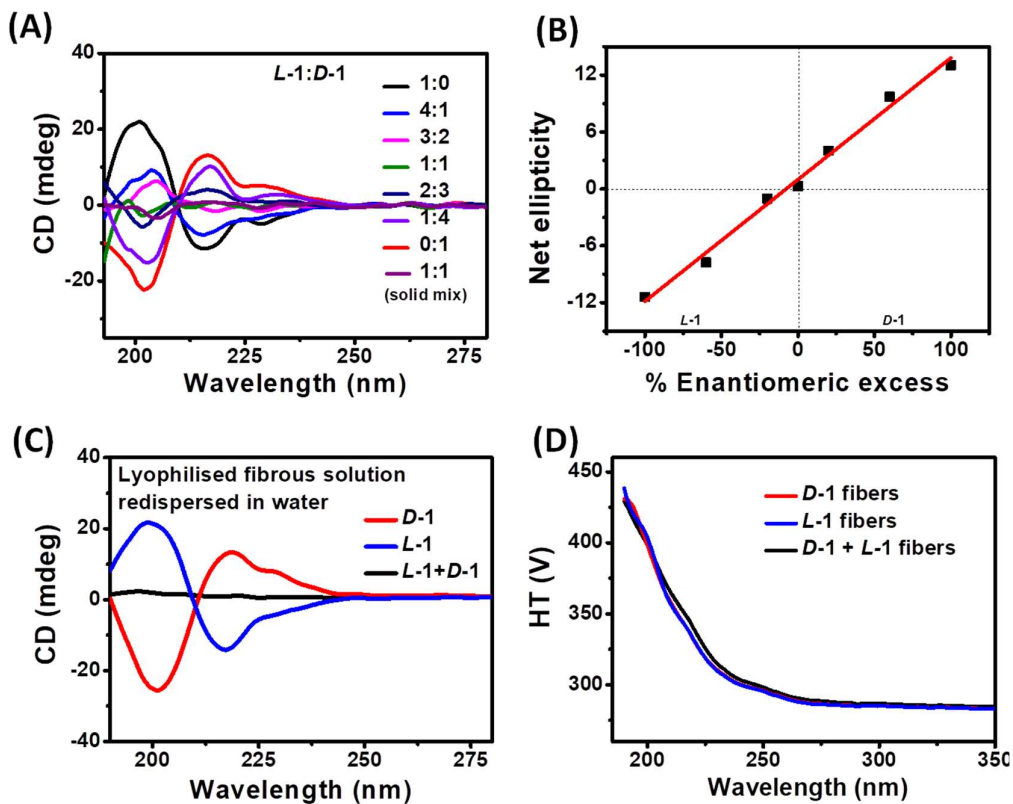


Figure S3: (A) CD spectra recorded for the mixture of peptides nanofiber solutions with different ratios of *L-1* and *D-1* (100 μ M) and equimolar solid phase mixing of *L-1* and *D-1* followed by dissolution in water. (B) Corresponding plot of net ellipticity at 216 nm with enantiomeric excess. (C) The peptide solutions in water were lyophilized to solid powder and CD spectra were recorded upon redispersing them in water. The redissolved peptide retains its chirality akin to the original peptide fibers. (D) HT voltage data of the CD spectra (100 μ M).

Thioflavin-T binding study:

Thioflavin-T (ThT) exhibits emission band at 480-500 nm upon binding to the ordered secondary structures of peptides ($\lambda_{ex} = 440$ nm). 2 μ L of ThT solution (50 μ M DMF stock) was added to 200 μ L of 0.4 mM aqueous peptide solution.

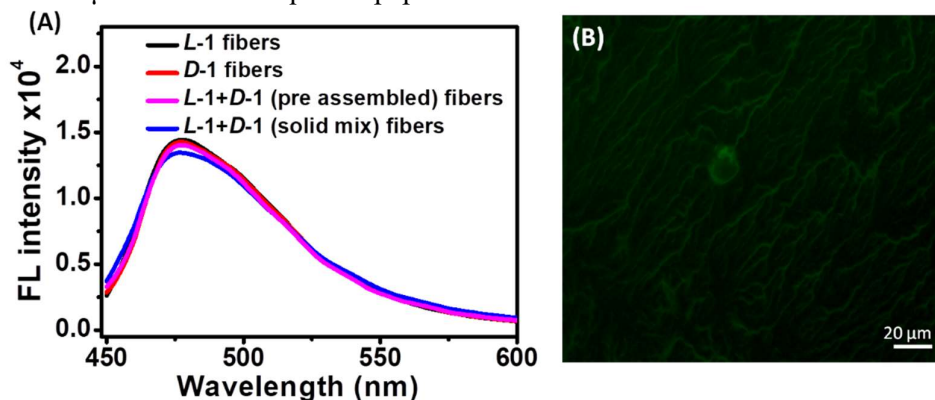


Figure S4: Fluorescence emission spectra as a consequence of ThT binding to *L-1* and *D-1* peptides and their mixture (1:1), both pre-assembled fibers' mixture and solid phase mixing followed by assembly. (B) Fluorescent imaging of ThT binding to mixture of *L-1* and *D-1* peptide fibers.

FT-IR studies

The peaks at 1625 cm^{-1} (amide I) and 1548 cm^{-1} (amide II) indicate the existence of parallel β -sheet. The peak associated with 1668 cm^{-1} is due to bound TFA counterions.

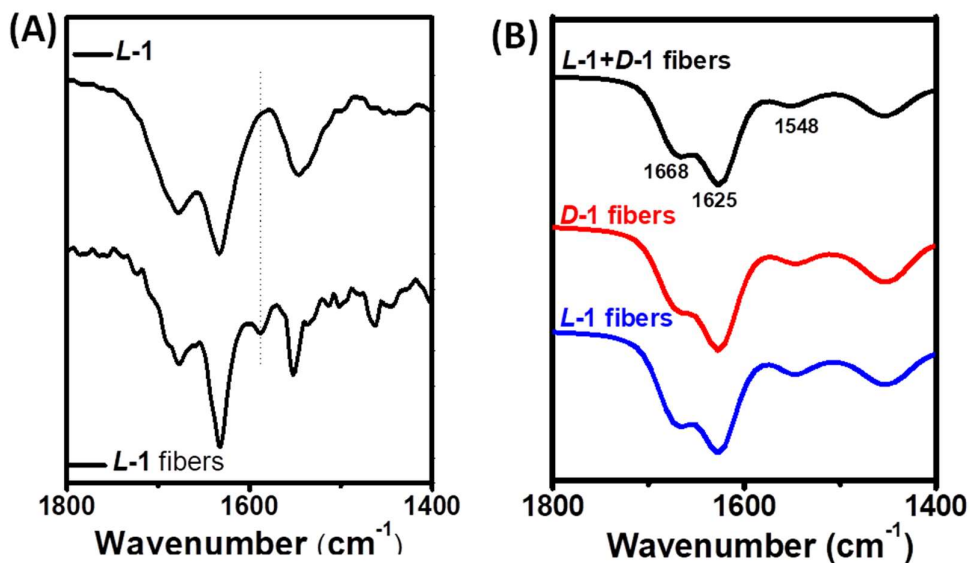


Figure S5: (A) FT-IR spectra for *L-1* peptide and *L-1* peptide nanofibers (after lyophilisation) with KBr pellet. (B) Parallel β -sheet in peptide solution *L-1*, *D-1* peptide nanofibers and their mixture in D₂O (5 mM).

Formation of hydrogel:

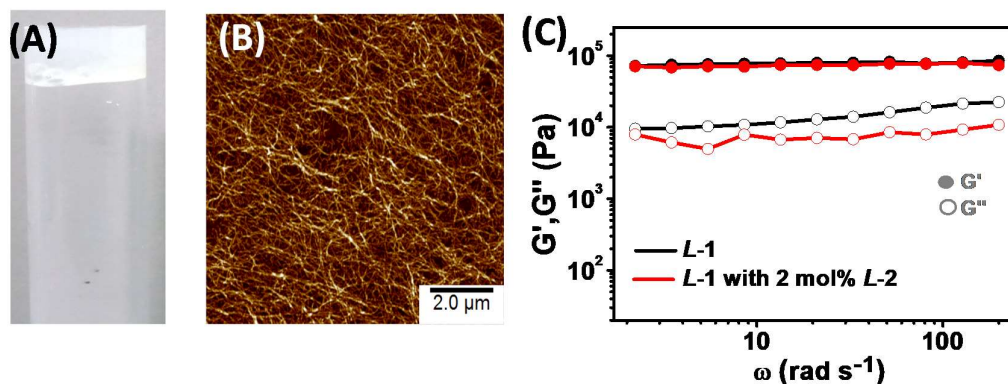


Figure S6: (A) digital picture of the hydrogel and (B) AFM imaging shows networked mesh of nanofibers in *L-1* + *D-1* gel (1 wt%). (C) Frequency sweep oscillatory rheology measurements for the hydrogels from *L-1* and *L-1* with 2 mol% *L-2* containing 2 v/v% DMSO.

UV-vis and Fluorescence Spectroscopy:

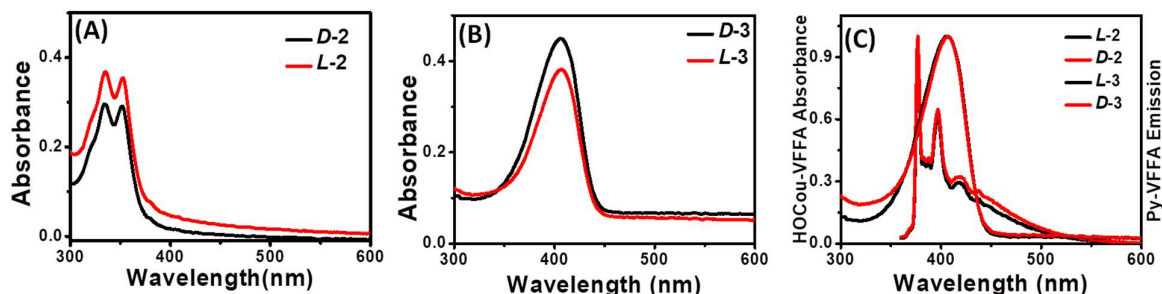


Figure S7: UV spectra of fluorescent peptides in Tris-HCl buffer (pH=7.4) (A) Pyrene based donor probe (*L-2* and *D-2*), (B) hydroxycoumarin based acceptor probe (*L-3* and *D-3*) (10 μ M) (stock was prepared in DMSO). (C) Overlap between the emission spectra of pyrene donor probe (*L-2* and *D-2* in *L-1* and *D-1* peptide solution respectively) and absorbance spectra of the hydroxycoumarin acceptor probe (*L-3* and *D-3* in *L-1* and *D-1* peptide solution respectively). This demonstrates the probes to be perfect FRET pair with a forster radius of 3.9 nm.⁴

100 μ L solution of *L-1* (100 μ M) and *D-1* (100 μ M) peptide nanofibers in tris-HCl buffer (pH=7.4) were mixed together to render each of their final conc. 50 μ M and final peptide concentration to be 100 μ M. Then 2 μ L of 50 μ M stock of *D-2* solution in DMSO was added (final concentration of fluorescent probe is 0.5 μ M; ratio of peptide to probe is 200:1) and the

mixture was vortexed and sonicated for 2 min in order to ensure the absence of excimer of pyrene molecule (~480 nm). Fluorescence spectra were recorded for the range of 360-600 nm and solution was excited at 347 nm. **D-3** (homochiral probe) or **L-3** (heterochiral probe) was added to the mixture (with increasing proportions of HOCou probe) followed by vortexing and sonication for 1 min to ensure the uptake of fluorescent peptides into the host peptide nanofibers. Energy transfer between the donor Py molecules to acceptor HOCou molecule increase the intensity at 450 nm and decrease the intensity of Py peak, which is the characteristics of FRET.

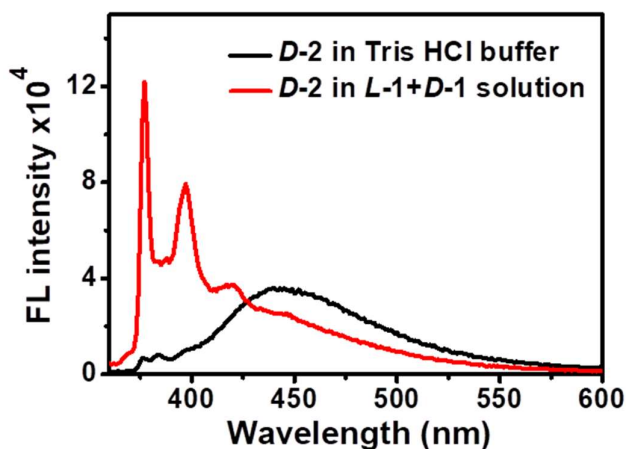


Figure S8: Pyrene excimer peak for **D-2** in tris-HCl buffer at 430-480 nm in the absence of host peptide and characteristic monomeric pyrene peak for **D-2** in the range of 375-410 nm in the presence of host peptide solution of **L-1** and **D-1**.

Förster energy-transfer efficiency (Φ_{ET}) was calculated by the following equation:

$$FRET\ Efficiency = \left(1 - \frac{F_{DA}}{F_D}\right) \cdot 100\%$$

F_D is the fluorescence intensity of the donor in the absence of the acceptor; F_{DA} is the fluorescence intensity of the donor in the presence of the acceptor.

The degree of self-sorting was estimated from as:

$$Self - sorting = \left(1 - \frac{Em_{Hetero} - Em_{Blank}}{Em_{Homo} - Em_{Blank}}\right) \cdot 100\%$$

Em values are emission intensities at the wavelength 450 nm. Percentage self-sorting is 84%.

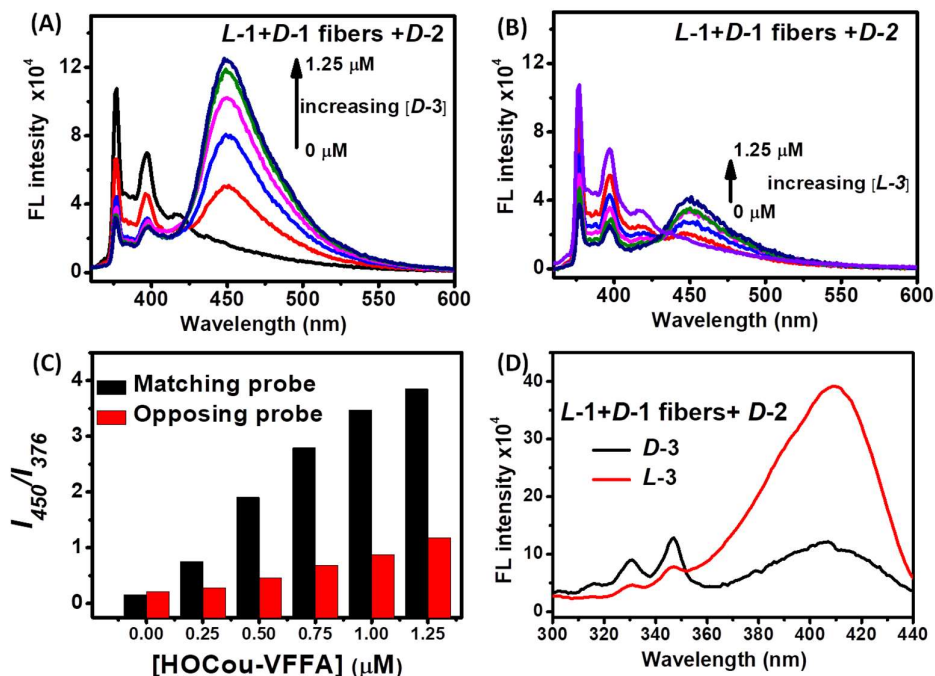


Figure S9: Changes in the emission spectra of of *L*-1 and *D*-1 peptide nanofibers solution (50 μM each) in Tris-HCl buffer (pH = 7.4); adding 2 μL *D*-2 (50 μM). (A) Homochiral case; increasing amount of *D*-3. (B) Heterochiral case; increasing amount of *L*-3. (Note: direct emission of hydroxycoumarin probe was subtracted from each graph) (C) FRET ratio (I_{450}/I_{376}) is increasing with acceptor concentration with significant difference in homochiral and heterochiral cases with matching and opposing chiral probes respectively. (D) The corresponding excitation scan with emission wavelength of 450 nm.

Measurement of kinetics of mixing for probe doped homochiral *L* nanofibers:

The rate constant, k , for the kinetic of mixing was determined by fitting the data to the first-order equation:

$$\ln\left(\frac{F_{max} - F_t}{F_{max}}\right) = -kt$$

Where F_t and F_{max} are the fluorescence intensities at 450 nm at times t and the maximum value obtained after the system have reached equilibrium. The negative slope of the line provides the apparent rate constant k .

Generation of Seed and seeded supramolecular polymerization:

500 μL of pre-assembled nanofibrous solution of **L-1** (1 mM) was probe sonicated using QSonica (model number Q700, power 700 watts and frequency 20 kHz) probe Sonicator using 4417 number microtip at an amplitude of 15% for ~ 5 minutes. The length of peptide nanofibers was determined using Image-J Software. 100 random fibers were selected from different areas of the images and a histogram was generated by choosing bin and frequency in Microsoft Excel. The average fiber lengths and PDI were estimated by calculating number average length (L_n) and weight average length (L_w) and the ratio polydispersity index (PDI) using eqs 1–3 respectively, where N_i is the number of fibers and of length L_i , and n is the number of fibers examined in each sample.

$$L_w = \frac{\sum_{i=1}^n N_i L_i^2}{\sum_{i=1}^n N_i L_i} \quad \text{--- (1)}$$

$$L_n = \frac{\sum_{i=1}^n N_i L_i}{\sum_{i=1}^n N_i} \quad \text{--- (2)}$$

$$PDI = \frac{L_w}{L_n} \quad \text{--- (3)}$$

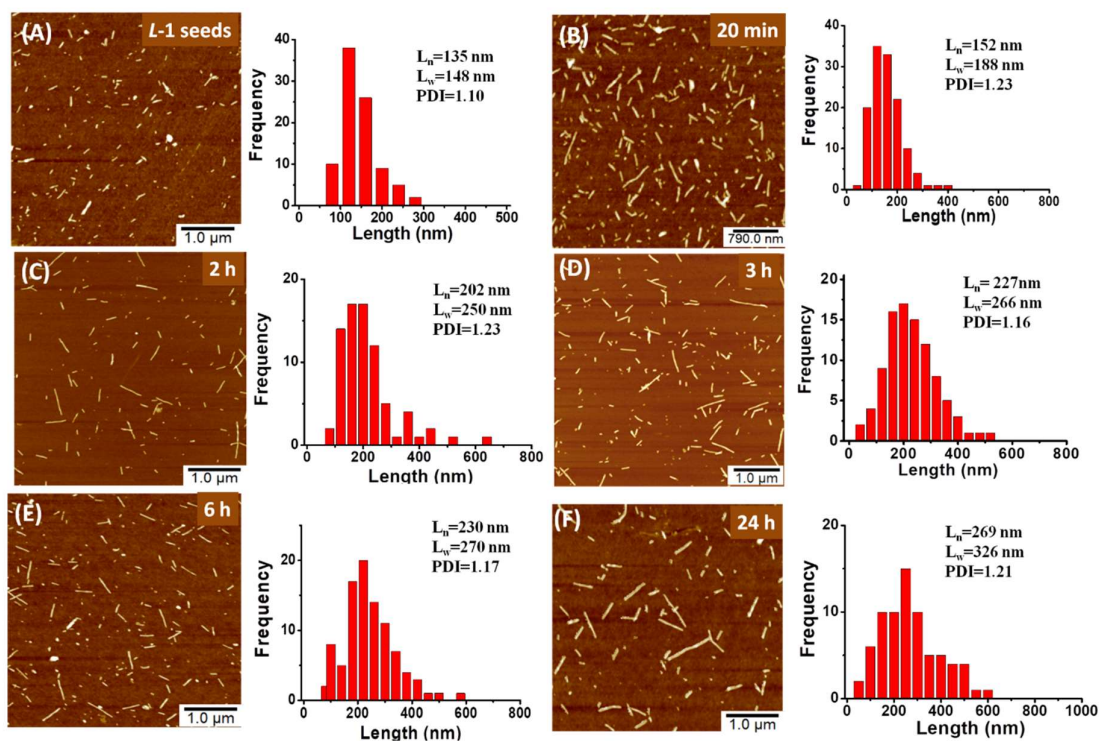


Figure S10: AFM height images and histogram length analyses for (A) **L-1** seeds and incubated **L-1** seeds with metastable nanoparticles of **L-1** and monitored after (B) 20 min, (C) 2 h, (D) 3h (E) 6 h and (F) 24h.

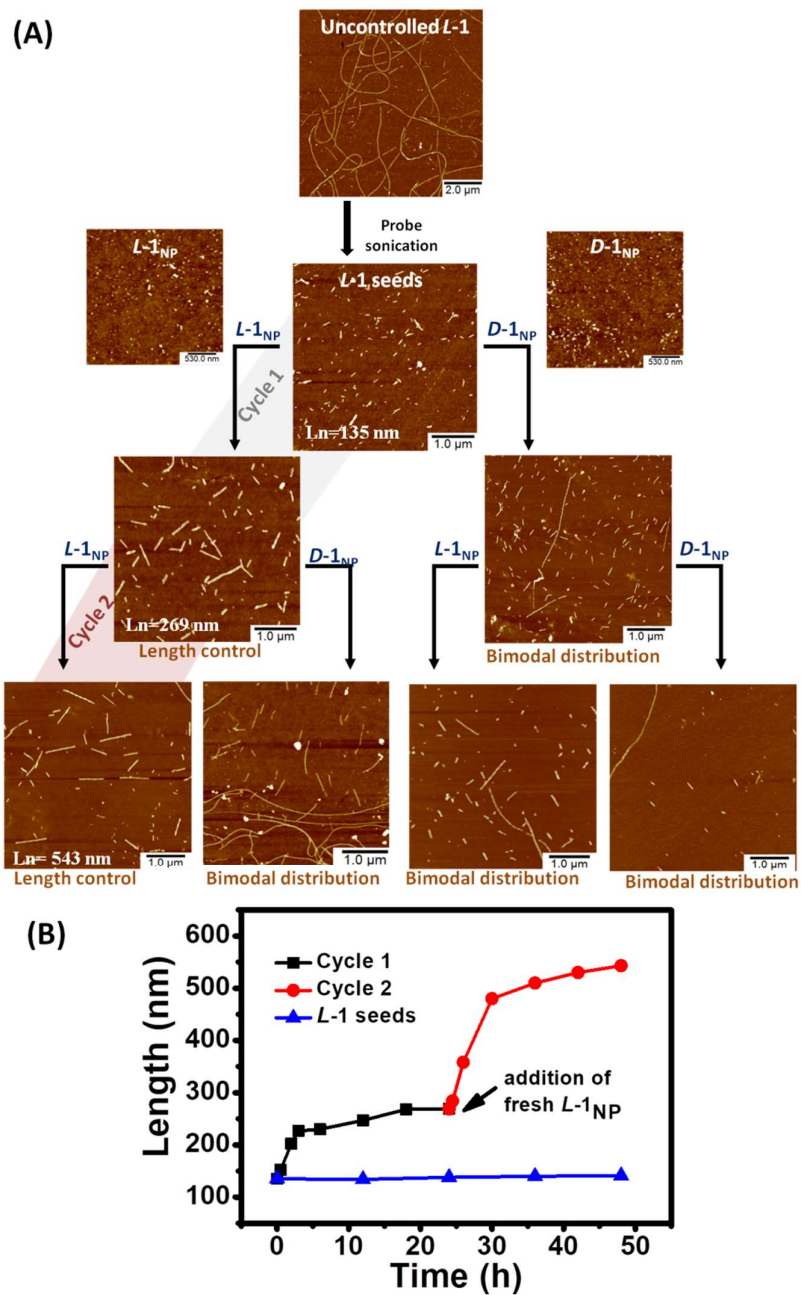


Figure S11: (A) Seeding (*L-1* seeds/*L-1* monomer) and cross-seeding (*L-1* seeds/*D-1* monomer) experiment monitored through AFM images show orthogonal assembly in heterochiral system and living nature of seeds for homochiral case. (B) Growth of *L-1* fiber seeds upon sequential addition of *L-1* monomer.

Seed mediated growth studies with ThT binding:

Kinetics of seed mediated growth of β -sheet forming nanofibers were monitored by ThT fluorescence in a continuous assay. Fluorescence readings (ex. 440 nm, em. 480 nm) were performed every 3 min with shaking for 1 s between readings for experiments; FL intensity at 480 nm was monitored for up to 250 min at 25 °C. For seeding and cross-seeding experiments, each well had 50 μ L of 100 μ M peptide seeds, 50 μ L of nanoparticle solution in 10% HFIP (100 μ M) and 0.4 μ M of ThT dye.

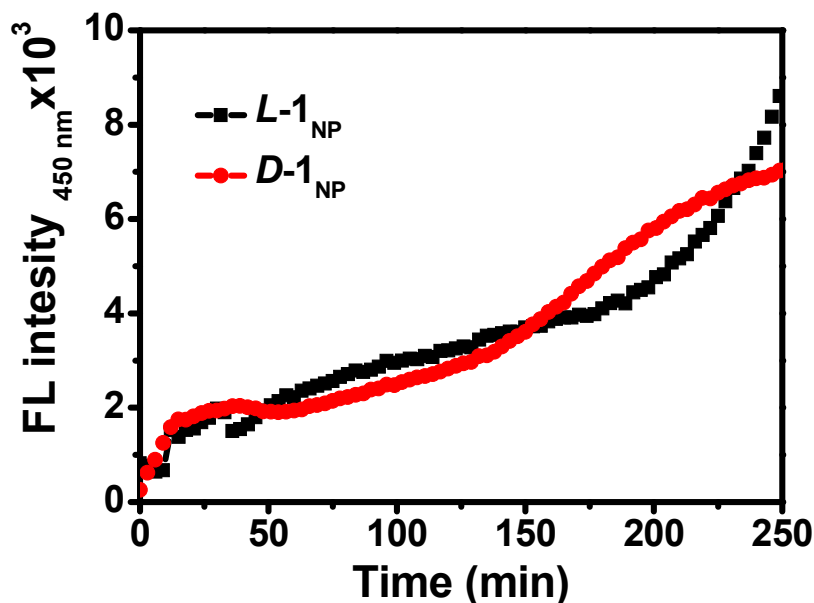


Figure S12: Growth of freshly dissolved solution of peptide amphiphiles (metastable nanoparticles) in 10 v/v% of HFIP-water (concentration = 100 μ M).

Confocal Laser Scanning Microscopy:

The nanofibrous solution stained with respective dye (30 μ L) was drop-casted on glass slide and covered with cover slip. The slides were kept at room temperature for overnight drying before imaging. The images were recorded with 488 nm and 561 nm laser excitation at 100X.

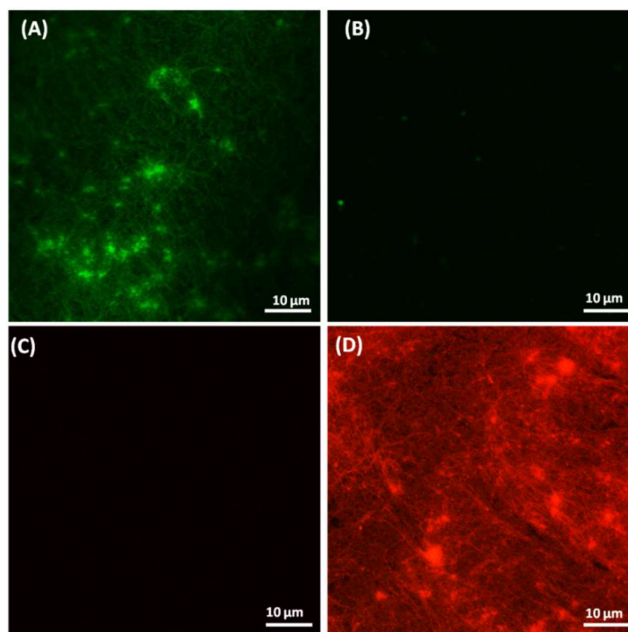


Figure S13: Confocal images of single-component fibres *L-1* (A) stained with *L-5* (B) *D-4*, (C) *D-1* stained with *L-5* and (D) *D-4* [peptide] = 1mM, [probe] = 1.5 μ M. The green and red images were acquired in 488 and 561 channels, respectively. The selective staining indicated on homochiral peptide probe stacks.

Super resolution Microscopy, Structured Illumination Method:

The appropriate concentration of self-assembled fibers (1: 100 (v/v) dilution from 0.4 mM stock) were taken in an eppendorf tube (PBS, pH 7.4). 10 μ L of above solution were dropcasted onto a glass slide. A clean coverslip was placed on top of it and proceed for fluorescence microscopy using structured illumination method.

The self-sorted fibers of *D* and *L*, (0.4 mM) were diluted in 100 μ L PBS, pH 7.4 (1:100 (v/v)) and kept in an eppendorf tube. 10 μ L of the solution were drop-casted onto a glass slide. A clean coverslip was placed on top of it and proceed for fluorescence microscopy using structured illumination method.

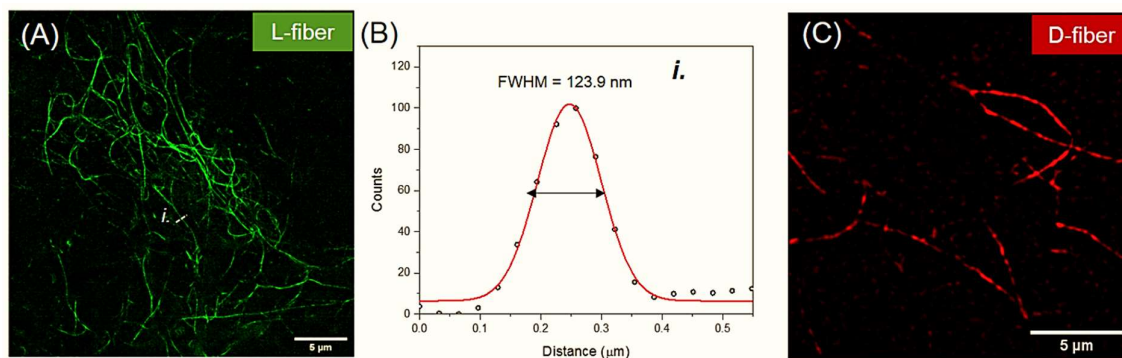


Figure S14: Super resolution structured illumination microscopic images of self-assembled fibers with fluorescent probe (A) **L-1** stained with **L-5** (C) **D-1** stained with **D-4** [peptide] = 40 μM , [probe] = 0.4 μM . (B) The diameter of the selected single green fiber (*i*) has been shown to be ~ 123 nm by SIM method. The green and red images were acquired in 488 and 561 channels, respectively. Fibers are visualized on staining with probes.

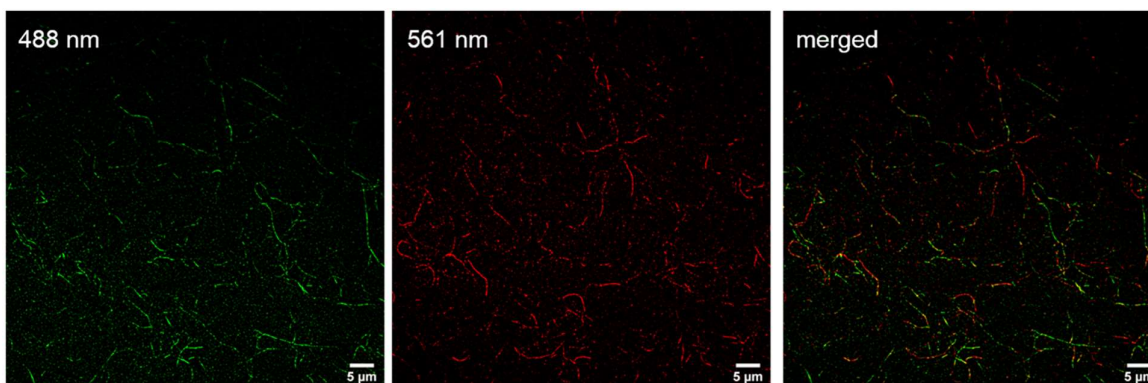


Figure S15: Super resolution structured illumination microscopy of four component mixture. 488 nm channel shows green fibers of **L-1** stained with **L-5**. 561 nm channel shows red fibers of **D-1** stained with **D-4**. Merged image represented chiral self-sorted self-assembled fibers with no overlapping of red and green fibers.

Enzymatic Responsiveness of the fibers:

The self-assembled fibers of **L-1** or **D-1** (0.5 mM) were incubated with chymotrypsin (10 μM) in phosphate buffer saline of pH = 7.4 at 37 $^{\circ}\text{C}$ for 5 h in sample vial and HPLC was recorded to explore emergence of new peak owing to proteolysis. The peak was characterized for the fragment peptides for the cleavage site by using HPLC-MS spectrometry. The HPLC chromatogram was recorded with acetonitrile and water (0.1% formic acid as additive) as mobile phase (gradient flow of 20 to 100% acetonitrile over 30 min, flow rate = 1 mLmin^{-1}). While **L-1** showed emergence of a new peak with retention time of 26 min and 24 min accounting for mass of 566 Da and 418 Da for the fragment species of $\text{C}_{10}\text{-VFF-COOH}$ and $\text{C}_{10}\text{-VF-COOH}$ fragment species, **D-1** exhibited proteolytic stability under similar conditions.

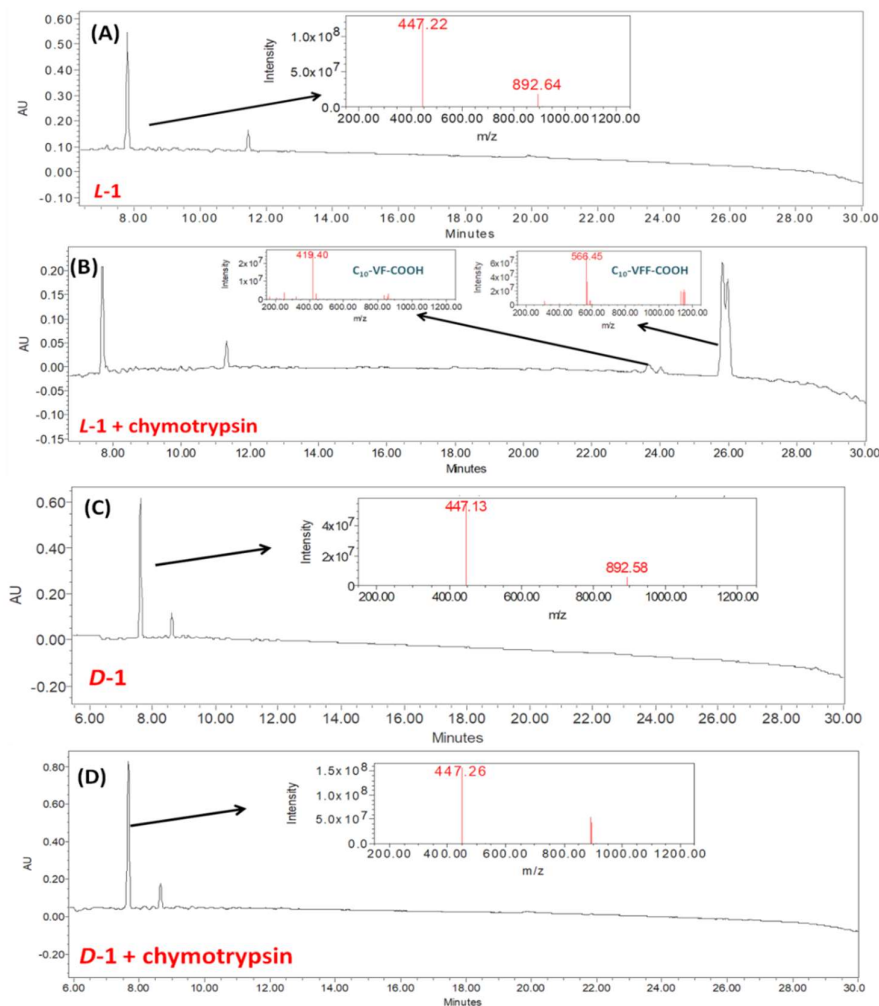


Figure S16: HPLC traces of **L-1** peptide (A) before and (B) 5 h after adding chymotrypsin showing peptide degradation. Mass traces of the peak at 26 min and 24 min shows presence of fragment accounting for amide bond breakage at the C-termini of phenylalanines (inset). HPLC traces of **D-1** peptide (A) before and (B) 5 h after adding chymotrypsin showing proteolytic stability for the **D-1** peptide. Peptide: enzyme = 50:1 incubated in PBS (pH= 7.4) at 37 °C for 5 h.

The fluorophore **L-5** showed the HPLC peak at 15.5 min accounting for the $[M+H]^+ = 984.44$ in mass spectra. However, upon incubation with chymotrypsin resulted a new peak at 17 min that indicates the proteolysis at the C termini of phenylalanines to give rise to a mass of 914 Da for the fragment species of FITC-C₆-VFF-COOH accounting for deletion of one alanine from the original peptide **L-5**.

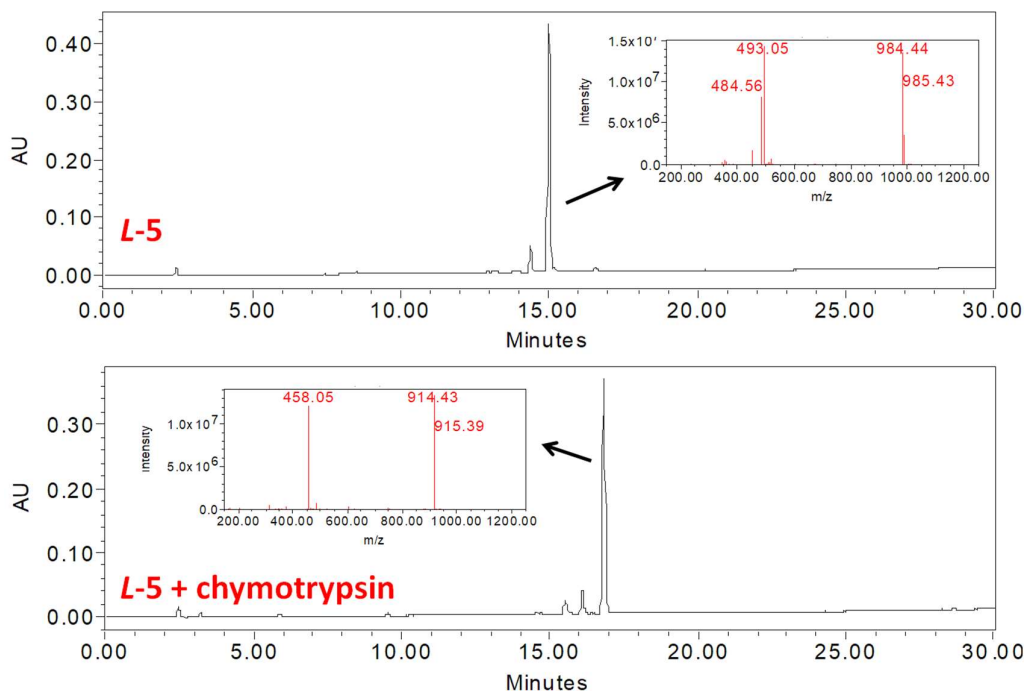


Figure S17: HPLC traces of *L-5* peptide (A) before and (B) 5 h after adding chymotrypsin showing peptide degradation. Inset of A shows mass trace for the peak at 15 min for *L-5* peptide. Inset of (B) shows mass traces of the peak at 17 min shows presence of fragment accounting for amide bond breakage at the C-terminus of phenylalanine (deleting one alanine amino acid).

For the single component system, the self-assembled fibers of *L-1* with *L-5* or *D-1* with *D-4* (100:1) were incubated with chymotrypsin (10 μ M) in phosphate buffer saline of pH = 7.4 at 37 $^{\circ}$ C for 5 h in an eppendorf tube (Peptide: Enzyme = 100:1). 10 μ L of above solution were drop-casted onto a glass slide. A clean coverslip was placed on top of it and proceed for fluorescence microscopy using structured illumination method.

L-1 peptide doped with *L-5* showed disappearance of green fiber observed through 488 channel (Figure S18A) indicating break down of the self-assembled fibers upon incubating the green fibers with chymotrypsin.

D-1 peptide doped with *D-4* exhibited red fibers through 561 nm channel. Upon incubating the red fibers (*D-1* peptide doped with *D-4*) with chymotrypsin for 5 hr, the red fibers showed proteolytic stability even after 5 h (Figure S18B).

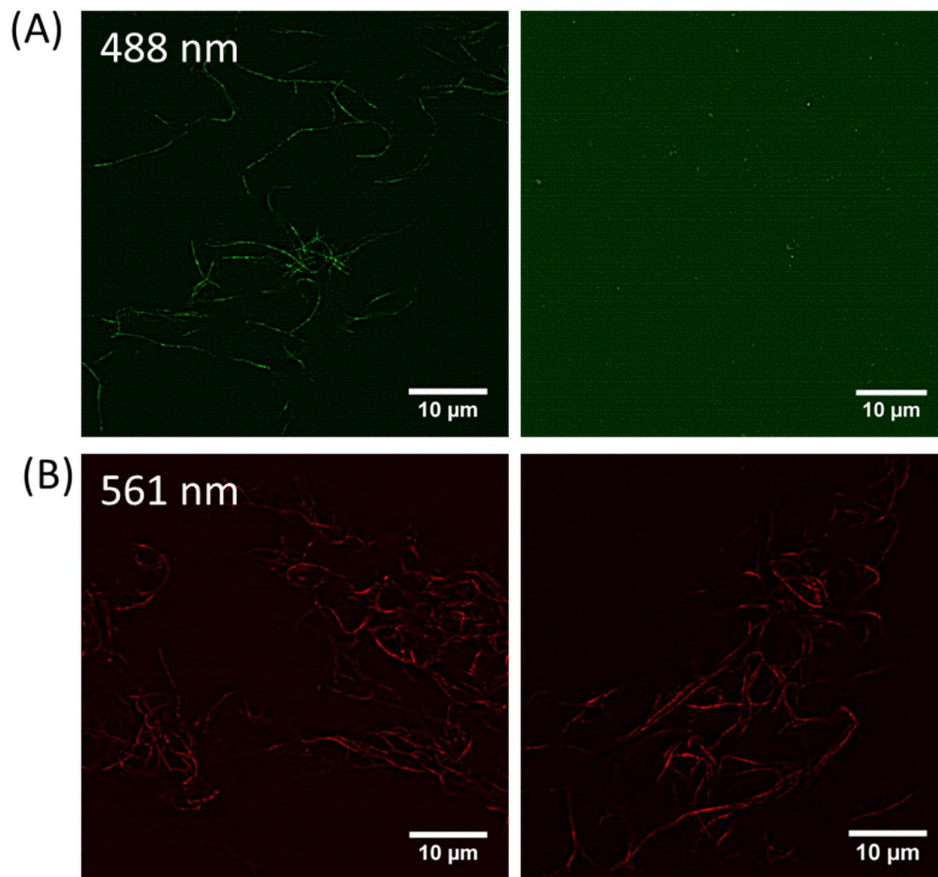


Figure S18: (A) SIM images of self-assembled *L-1* fibers stained with green fluorescent probe *L-5* incubated without (left) and with (right) chymotrypsin for 5 h in PBS (pH= 7.4) at 37 °C (Upper panel show images acquired in green channel, 488 nm). Upper right images does not show any nanofibers in green channel, suggesting complete degradation of the *L*-peptides. (B) SIM images of self-assembled *D-1* fibers stained with red fluorescent probe *D-4* incubated without (left) and with (right) chymotrypsin for 5 h in PBS (pH= 7.4) at 37 °C. Lower right image shows presence of red fibers indicating proteolytic stability *D*-peptides. Peptide: enzyme = 100:1.

For the four component system, the self-sorted fibers of *L-1* with *L-5* or *D-1* with *D-4* (100:1) were incubated with chymotrypsin (10 μM) in phosphate buffer saline of pH = 7.4 at 37 °C for 5 h in an eppendorf tube. 10 μL of above solution were drop-casted onto a glass slide. A clean coverslip was placed on top of it and proceed for fluorescence microscopy using structured illumination method.

Upon incubating with enzyme, the *D*-fibers are stable as visualized from 561 nm channel. However, green emission appeared from red fibers only, supported by high overlap coefficient value as merged channel. No separate green *L-1/L-5* fibers were observed. *L-1* and *L-5*

underwent proteolytic hydrolysis at the C-termini of phenylalanine. The fragment species from **L-5** has a negatively charged COO⁻ group at C-termini pH= 7.4, that interact with the positively charged **D-1** fibers.

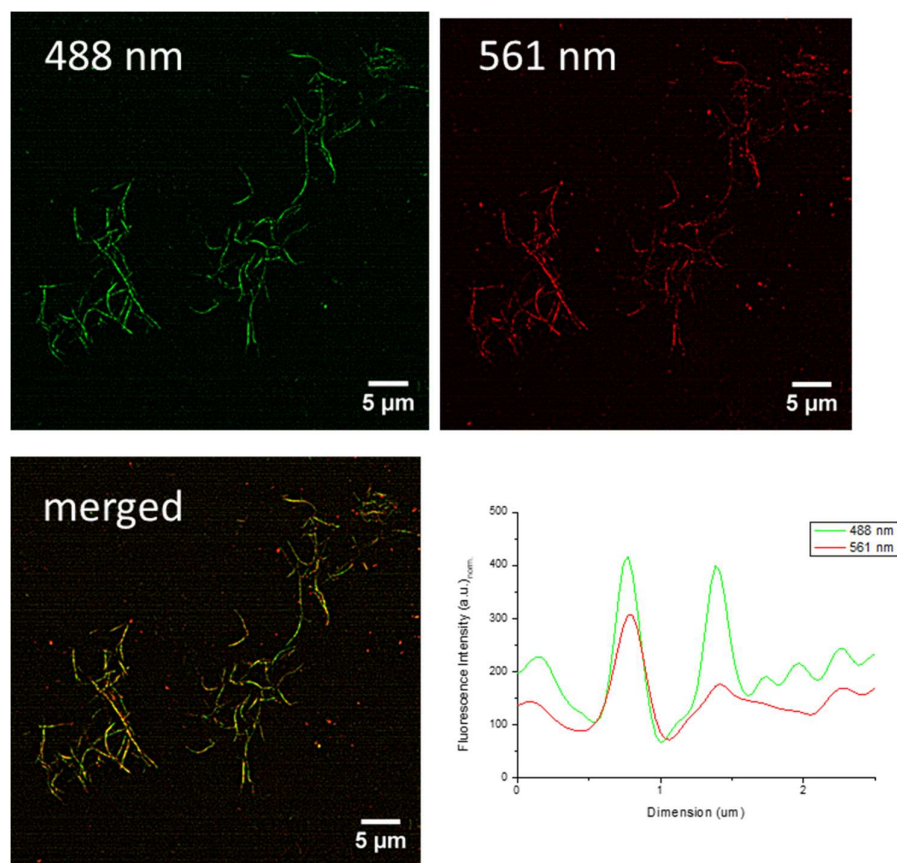


Figure S19: SIM images of four component system containing self-sorted **D-1** fibers stained with red fluorescent probe **D-4** and **L-1** fibers stained with green fluorescent probe **L-4** after incubating with chymotrypsin for 5 h in PBS (pH= 7.4) at 37 °C. Peptide: enzyme = 100:1. (A-D) show images acquired in green, red, merged channel and fluorescent intensity for the **D-1** fibers with green **D-4** in absence and in presence of chymotrypsin.

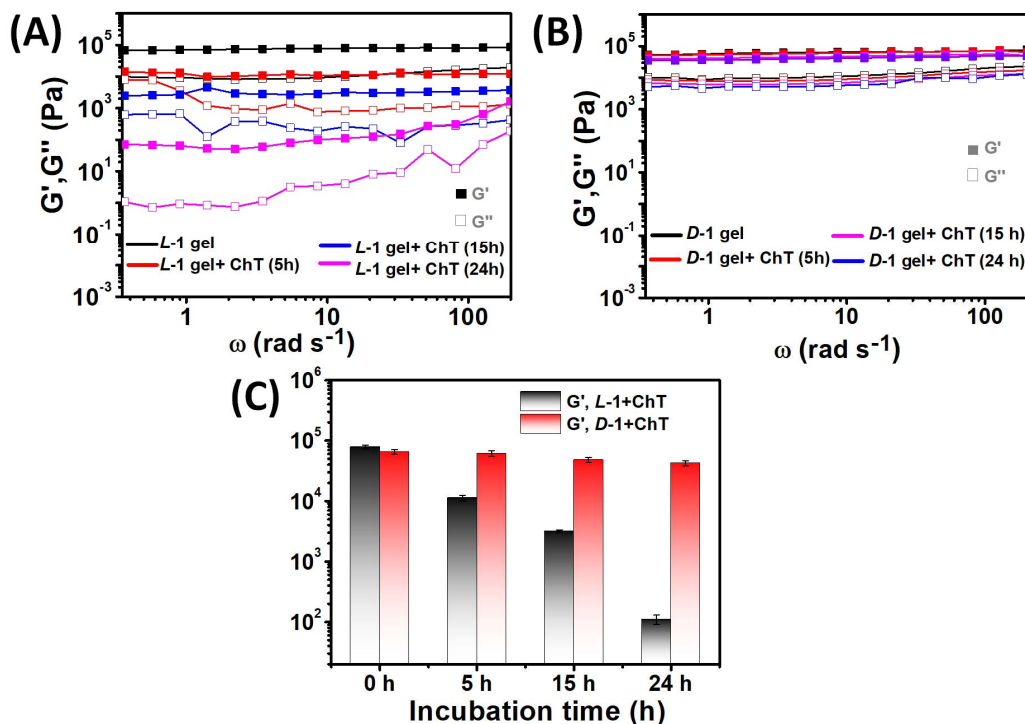


Figure S20: Oscillatory frequency sweep measurements for the hydrogels from (A) *L-1* and (B) *D-1* amphiphiles upon incubation with chymotrypsin for 0, 5, 15 and 24 h at 37 °C in phosphate buffer of pH 7.4. (C) Bar diagram demonstrates the gradual decrease in G' values for *L-1* hydrogels while G' values for *D-1* hydrogels stayed almost unchanged upon chymotrypsin mediated enantio-selective hydrogel degradation. [Peptide]: [Enzyme] = 100:1 peptide concentration = 10 mM.

References:

1. D. R. Bolin, I. I. Sytwu, F. Humic and J. Meienhofer *Int. J. Peptide Protein Res.*, 1989, **33**, 353.
2. K. F. Chilvers, J. D. Perry, A. L. James and R. H. Reed, *J. Appl. Microbiol.* 2001, **91**, 1118.
3. M. Jullian, A. Hernandez, A. Maurras, K. Puget, M. Amblard, J. Martinez and G. Subra, *Tetrahedron Lett*, 2009, **50**, 260.
4. P. Wu and L. Brand. *Anal. Biochem.* 1994, **218**, 1-13.